Protein rotational dynamics investigated with a dual EPR/optical molecular probe

Spin-labeled eosin

Charles E. Cobb, Eric J. Hustedt, Joseph M. Beechem, and Albert H. Beth
Molecular Physiology and Biophysics, Vanderbilt University, Nashville, Tennessee 37232-0615 USA

ABSTRACT An acyl spin-label derivative of 5-aminoeosin (5-SLE) was chemically synthesized and employed in studies of rotational dynamics of the free probe and of the probe when bound noncovalently to bovine serum albumin using the spectroscopic techniques of fluorescence anisotropy decay and electron paramagnetic resonance (EPR) and their long-lifetime counterparts phosphorescence anisotropy decay and saturation transfer EPR. Previous work (Beth, A. H., Cobb, C. E., and J. M. Beechem, 1992. Synthesis and characterization of a combined fluorescence, phosphorescence, and electron paramagnetic resonance probe. Society of Photo-Optical Instrumentation Engineers. Time-Resolved Laser Spectroscopy III. 504–512) has shown that the spin-label moiety only slightly altered the fluorescence and phosphorescence lifetimes and quantum yields of 5-SLE when compared with 5-SLE whose nitroxide had been reduced with ascorbate and with the diamagnetic homolog 5-acetyleosin. In the present work, we have utilized time-resolved fluorescence anisotropy decay and linear EPR spectroscopies to observe and quantitate the psec motions of 5-SLE in solution and the nsec motions of the 5-SLE-bovine serum albumin complex. Time-resolved phosphorescence anisotropy decay and saturation transfer EPR studies have been carried out to observe and quantitate the μsec motions of the 5-SLE-albumin complex in glycerol/buffer solutions of varying viscosity. These latter studies have enabled a rigorous comparison of rotational correlation times obtained from these complementary techniques to be made with a single probe. The studies described demonstrate that it is possible to employ a single molecular probe to carry out the full range of fluorescence, phosphorescence, EPR, and saturation transfer EPR studies. It is anticipated that "dual" molecular probes of this general type will significantly enhance capabilities for extracting dynamics and structural information from macromolecules and their functional assemblies.

INTRODUCTION

There is an extensive scientific literature describing the use of exogenous molecular probes in studies of the structures, orientational properties, and/or dynamics of biological macromolecules. Spectroscopic techniques which have relied heavily on the use of exogenous probes include electron paramagnetic resonance (EPR) and fluorescence, as well as their long-lifetime counterparts of saturation transfer EPR (ST-EPR) and phosphorescence. In the case of EPR and ST-EPR, the most common approach of experimentalists has been to introduce a stable nitroxide spin-label (2, 3) into the system under investigation as a unique reporter probe. Similarly, fluorescent and phosphorescent dyes exhibiting widely varying absorption and emission properties have been synthesized in many molecular forms which are suitable for labeling of a specific component or selected components of a macromolecular assembly. A representative bibliography of spin-label and luminescent probes which have been synthesized and studies in which they have been employed during the past two decades has been compiled by Haugland (4).

Experimentalists using EPR or fluorescence spectroscopies in conjunction with exogenous probes have most often chosen one of the techniques, and then proceed to identify a suitable probe and to establish its location or reaction site(s) on a biomolecule. Rarely have investigators invested the time necessary to label a single system with a spin-label probe for EPR studies and with a fluorophore for fluorescence studies at a common site, even though these two techniques would often provide complementary information, as recently discussed for ST-EPR and transient phosphorescence emission anisotropy by Thomas (5) and by Burghardt and co-workers for EPR and fluorescence (6–8). Even in those instances where spin-label and fluorescent/phosphorescent probes are available with the same reactive group (e.g., maleimide, iodoacetamide, or isothiocyanate), substantial differences in the physicochemical properties of the probe molecules themselves often lead to different labeling specificities on target macromolecules. However, as more sophisticated questions about the role of molecular motions and/or changes in orientational distributions of molecules in regulating functions have arisen, it has become clear that it is desirable to observe the systems using as many complementary approaches as possible.

The problem of having to label with two different probes could be circumvented, in theory, if a single probe could be synthesized which possessed both an unpaired electron for EPR/ST-EPR detection and a suitable chromophore for fluorescence/phosphorescence detection. One approach which has recently been employed by Ajtai and Burghardt (7) is to generate a transient π-radical by photochemical reduction of eosin, erythrosin, or fluorescein and to carry out EPR studies on this radical during its transient lifetime while carrying out complementary optical studies on samples contain-

Address correspondence to Albert H. Beth, Molecular Physiology and Biophysics, 727 Light Hall, Vanderbilt University, Nashville, TN 37232-0615.

0006-3495/93/03/605/09 $2.00

ing the nonreduced chromophore. This is a potentially powerful approach for those systems in which the radical persists for sufficient time to permit collection of EPR spectra with adequate signal-to-noise.

A second approach would be to employ a stable nitroxide coupled to a luminescent probe as the EPR reporter group. Unfortunately, paramagnetic centers are known to be effective collisional quenchers of fluorescence and phosphorescence, suggesting that the desired optical properties of such a stable "dual probe" might be compromised. Indeed, there is a sizable literature describing the effects of spin-label centers on optical properties of a variety of probes (e.g., 9, 10). However, Stryer and Griffith (11) synthesized a dansylated spin-label probe which served as an EPR reporter and also maintained a reasonable fluorescence quantum yield. In previous work (1), we reported the synthesis and characterization of a spin-labeled derivative of 5-aminoeosin which exhibited the desired dual (EPR and optical) reporter characteristics. We have now synthesized a [^{15}N,^{2}H]-spin-labeled analogue of 5-aminoeosin and have employed it in a series of studies aimed at observing and quantitating the rotational diffusion of this probe in solution and when noncovalently complexed with bovine serum albumin in solutions of varying viscosity. The results obtained indicate that it is possible to carry out the full range of fluorescence, EPR, phosphorescence, and ST-EPR studies using this dual molecular probe and that an internally consistent description of the rotational dynamics of albumin is provided by independent analyses of the resulting data sets. Additionally, we have developed a computational approach for global nonlinear analysis of EPR and optical data from these dual probes as described in the accompanying manuscript (12).

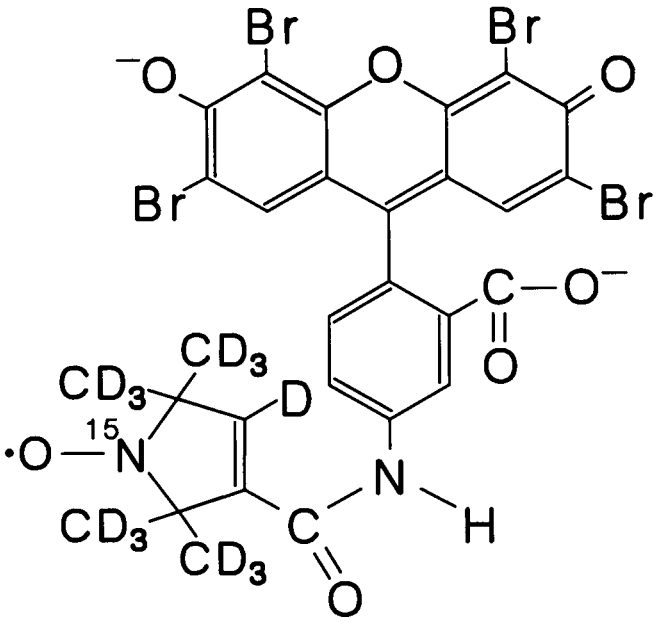

FIGURE 1 Chemical structure of [^{15}N,^{2}H$_{13}$]-5-SLE.

METHODS

Synthesis and purification of 5-SLE

5-Aminoeosin (hydrochloride) was obtained from Molecular Probes (Eugene, OR) and converted to the free amine disodium salt form by neutralization in water with NaOH, followed by lyophilization and removal of the NaCl by silica gel column chromatography using HPLC-grade methanol as the eluent. 2,2,5,5-Tetramethyl-3-pyrroline-d_{13},1-^{15}N-1-oxyl-3-carboxylic acid was obtained from MSD Isotopes (Montreal, Canada) and was converted to the anhydride using published procedures (13). Dimethyl formamide (DMF; Fisher Scientific) was dried over 3 Å pore size molecular sieves prior to use. Other reagents and solvents were obtained from standard commercial sources in reagent grade and used without further purification.

The disodium salt of 5-aminoeosin was dried in vacuo at 185°C for 1 h followed by addition of the spin-label anhydride (1.2 mol anhydride/mol 5-aminoeosin). The reactants were dissolved in dry DMF, the flask purged with argon, and sealed with a $CaCl_2$ drying tube. The sample was slowly heated to 60°C with gentle stirring, kept at this temperature for one hour, and then cooled to room temperature. The DMF was removed via rotary evaporation.

The 5-SLE product (Fig. 1) was purified by preparative thin layer chromatography (TLC). The sample was dissolved in HPLC-grade methanol, applied to a silica gel TLC plate (1,000 μm thick; Whatman, Maidstone, England), and the plate developed using methanol:chloroform:ammonium hydroxide (48:48:4 vol:vol:vol) as the mobile phase. Unreacted 5-aminoeosin ran close to the origin ($R_f \sim 0.2$), and the 5-SLE product ran further up the plate ($R_f \sim 0.7$), well separated from the unreacted spin-label ($R_f \sim 0.9$). The 5-SLE band was scraped from the plate and the product solubilized out of the silica with methanol, vacuum filtered through a 0.2 μm nylon filter, and the methanol removed under reduced pressure. The residue was redissolved in a minimal volume of deionized water, converted to the Na^+ form (Bio Rad AG50W-X8 cation exchange column, Na^+ form; Richmond, CA), and lyophilized to yield a fluffy red solid. Analytical TLC of the purified 5-SLE gave a single spot of $R_f \sim 0.7$ (same mobile phase as above). The molecular weight of the purified product was determined by mass spectrometry (FB+ mode, 20% glycerol in DMSO matrix). The spin density (moles of free radical/mole of compound) was calculated by quantitating the number of nitroxides in a 5-SLE sample by double integration of its first derivative EPR spectrum (using 2,2,5,5-tetramethylpyrrolin-1-oxyl-3-carboxylic acid as a spin-label standard) and the dry weight of the product.

Collection and analyses of EPR spectra

EPR and ST-EPR spectra were collected using a Bruker ESP-300 spectrometer system operating at X-band as described previously (15). Samples were contained in a quartz EPR flat cell (Wilmad WG-813; Buena, NJ) for recording all spectra. Sample temperature was set and maintained via a Bruker ER 4111VT temperature controller by blowing precooled nitrogen gas through the front optical port of the microwave cavity. The modulation amplitude and the effective microwave observer power at the sample were measured using peroxylamine disulfonate as described previously (16). Bovine serum albumin (BSA, fraction V; Sigma Chemical Co., St. Louis, MO) was used without further purification. Experimental data were analyzed by computer modeling of EPR line shapes as described in previous work (17, 18). The best-fit was determined by maximization of the r^2-statistic for a given model. All calculations of EPR and ST-EPR spectra were carried out on an Ardent Titan computer running under the UNIX operating system.

Collection and analysis of fluorescence and phosphorescence data

All samples (3 ml) for phosphorescence measurements were purged of molecular oxygen by blowing a stream of argon onto the surface of the solution in the cuvette for 15 min. In addition, they contained an enzymatic oxygen removal system consisting of 100 μg/ml glucose oxidase, 15 μg/ml catalase, and 5 mg/ml glucose (19). Glucose oxidase and catalase were obtained from Sigma Chemical Co. (St. Louis, MO). The concentration of 5-SLE used in the optical measurements (1.5 μM) was such that the absorption at the excitation wavelength used did not exceed 0.1 AU (either free or bound to BSA).

The fluorescence emission spectrum of 5-SLE was recorded using a 75 W xenon-arc light source (Oriel, Stratford, CT) and monochrometer set to 520 nm excitation wavelength (4 nm bandwidth), with the fluorescence emission detected via a 512 channel optical multi-channel analyzer (Princeton Instruments, Trenton, NJ). The fluorescence decay data were collected using the 292.5 nm output from a Coherent model 702 dye laser (the dye used was Rhodamine 6G, frequency doubled, model 7220 cavity dumper) synchronously pumped by a Coherent Antares 76-S Nd:YAG laser (Palo Alto, CA) as the excitation source, with detection of the fluorescence decay by time-correlated photon counting using a 6 μm Hamamatsu microchannel plate detector. The instrument response function was 60-120 psec FWHM. A 520 nm interference filter (#54351; Oriel Corp., Stratford, CT) in the emission path was employed to reduce background and scattered light. A zero-order one half wave plate in a rotation stage (Newport Corp., Fountain Valley, CA) was employed to rotate the excitation polarization for accurate determination of the G-factor for correction of the anisotropy decay curves due to polarization bias of the detection instrumentation.

Phosphorescence spectra were recorded using a Coherent Antares 76-S CW Nd-YAG laser in Q-switch mode (frequency doubled to 532 nm) as the excitation source. The excitation beam was routed to the sample compartment and the peak power of the excitation beam was attenuated by neutral density filters (Oriel Corp.) inserted in the excitation path to prevent photobleaching of the sample (no decrease in the phosphorescence emission intensity was observed over the course of data collection). The repetition rate of the laser pulses was kept at a low level (80 to 120 Hz) to allow decay of the eosin phosphorescence before another excitation pulse impinged on the sample. Collection of the phosphorescence emission spectrum was accomplished by positioning a 580 nm cut-on glass filter (Hoya Optics) in the sample chamber emission arm between the sample cuvette and an American Holographic DB10 double monochrometer. For collection of phosphorescence decay and anisotropy data, a 640 nm cut-on glass filter (Hoya Optics) was employed, and the monochrometer was eliminated. The emission photons were detected via a Hamamatsu R928 photomultiplier tube in single photon counting mode housed in a Hamamatsu C1392-08 gated photomultiplier tube base (gate voltage used was 250 V). The gate width and delay were controlled by a Tennelec (Oak Ridge, TN) gate and delay generator using the external sync output from the laser Q-switch as a trigger and set to the minimal level required to gate the PMT during the laser pulse. The PMT output signal was amplified by a Stanford Research Systems SR445 300 mHz amplifier and passed to a Stanford Research Systems SR430 multichannel scalar. Phosphorescence decay data were collected in 40 nsec wide bins (15,360 bins; total decay time recorded was 614 μs), and collection time was approximately 6 min per spectrum. The G-factors, determined either by tail matching or by 90° excitation rotation, ranged from 0.99 to 1.02. Sample temperature was set and maintained by running water from a refrigerating/heating water bath through the water jacket of the cuvette holder.

The fluorescence and phosphorescence anisotropies (r) were calculated from the fluorescence or phosphorescence emission intensity decay curves measured parallel and perpendicular to the vertically polarized excitation source ($I_\parallel$ and $I_\perp$, respectively) and their G-factors by the equation:

$$r(t) = (I_\parallel - GI_\perp)/(I_\parallel + 2(GI_\perp)). \quad (1)$$

The resulting fluorescence and phosphorescence anisotropy data were fit to a sum of exponential terms (see accompanying manuscript (12)):

$$r(t) = \sum_i \alpha_i e^{(-t/\phi_i)}, \quad (2)$$

using a nonlinear least-squares routine (Marquardt-Levenberg algorithm) (20, 21), running on an IBM 80486 compatible computer. For the case of isotropic rotational diffusion and in the absence of complicating factors, $\phi = \tau_r$, where τ_r is the rotational correlation time. In the case when the anisotropy did not go to zero in the accessible experimental time frame (e.g., the fluorescence anisotropy of the 5-SLE-BSA complex), a constant term (r_∞) was added to Eq. 2 to adequately fit the data.

RESULTS

Synthesis and optical properties of 5-SLE

The 5-aminoeosin starting material was nearly quantitatively converted to the spin-labeled product during the reaction, and was easily purified by TLC. We also attempted to purify the 5-SLE using reverse phase HPLC; however, we were unable to find suitable conditions which resulted in acceptable recovery of the material injected onto the HPLC column. The spin density of 5-SLE was ~0.95 nitroxide spins per eosin molecule (determined as described in the Methods section above). The mass spectroscopy analysis indicated molecular ions of 874 and 896 mass units, consistent with the calculated molecular weights of the disodium salt of 5-SLE ([^{14}N,^{1}H] spin label derivative) plus a proton or a sodium ion, respectively.

The absorption, fluorescence emission, and phosphorescence emission spectra of 5-SLE are shown in Fig. 2. These optical properties (as well as the absorption extinction coefficient and the fluorescence and phosphorescence lifetimes and quantum yields) of 5-SLE were essentially the same as those of the acetylated eosin derivative and those of 5-SLE whose nitroxide had been reduced by ascorbate (1), indicating that the nitroxide radical had a minimal effect on the optical spectroscopic properties of the eosin. The absorption maximum of 5-SLE shifts from 518 to 530 nm upon binding to BSA, and the extinction coefficient increases by less than 10%, which is consistent with the findings of Cherry et al. (22) for eosin-5-isothiocyanate binding to BSA.

EPR and fluorescence emission anisotropy of 5-SLE in solution and bound to BSA

The linear EPR spectrum of 5-SLE in buffer is shown in Fig. 3 (*top spectrum*). The sharp two-line spectrum observed was consistent with a ^{15}N nitroxide spin label tumbling in the motional narrowing time window for linear EPR. Superimposed on this spectrum is a calculated line-shape generated using an isotropic rotational

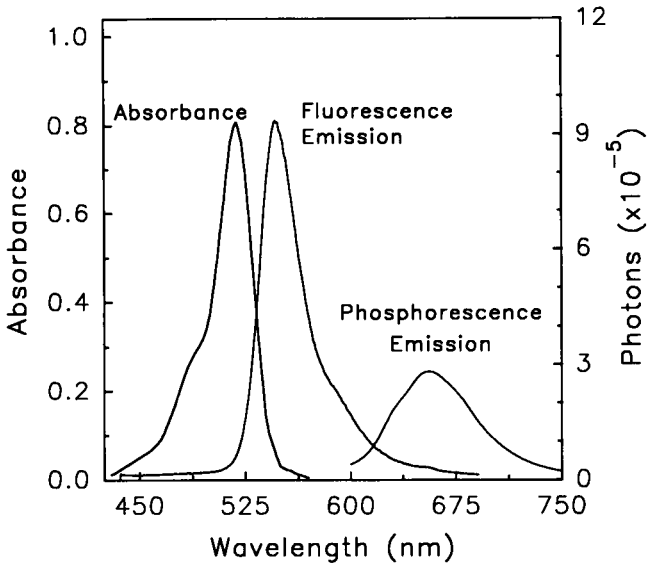

FIGURE 2 Absorption, fluorescence emission, and phosphorescence emission of 5-SLE. The sample composition was 1.5 μM 5-SLE in 5 mM sodium phosphate pH 8.0 (sample was deoxygenated for the phosphorescence measurement as described in Methods). The absorption spectrum was recorded on a Beckman DU-7 spectrophotometer. The fluorescence and phosphorescence emission spectra are not to scale.

correlation time (τ_r) of 150 ps. Upon binding to BSA at 20°C, the spectrum changed markedly (Fig. 3, *bottom*) into a composite line shape which was dominated by the slow motion of the 5-SLE/BSA complex. The spectrum was resolved into two motional components whose simulated fits are superimposed on the original composite spectrum. The major component (*dotted line*) was fit by a calculated spectrum with τ_r set to 30 ns, which agreed well with the τ_r of BSA in aqueous solution at 20°C based upon the hydrated radius calculated below from ST-EPR and transient phosphorescence anisotropy, and from the hydrodynamically determined hydrated radius (23). The minor component (*dot-dashed line*) was reasonably fit by a calculated spectrum having a τ_r of 3 ns. The almost complete disappearance of the sharp two line spectrum of free 5-SLE indicated that virtually all of the 5-SLE was bound to BSA under the experimental conditions employed.

The fluorescence anisotropy decay curve of 5-SLE in buffer (excited into the negative polarization band at 292.5 nm) is shown in Fig. 4 (fast decaying curve). The decay curve was well fit with a single exponential term having a ϕ of 0.43 ns, as indicated by the residuals from the fit in the bottom panel. The initial anisotropy value observed was approximately −0.13, compared to a theoretical rigid limit value of −0.2. Since the fluorescence lifetime of 5-SLE in solution was approximately 0.9 ns, this ϕ was determined with high accuracy (for comparison, a ϕ of 0.55 ns has been reported for eosin in water) (24). There was a marked change in the anisotropy curve when the 5-SLE was bound to BSA, as shown in the slow decaying curve in Fig. 4. This curve was best-fit with a single exponential equation containing a large r_∞ term, as indicated by the residuals from the fit in the bottom panel. The fast rotational time component (ϕ = 4.7 ns) correlated reasonably well with the minor component of the EPR spectrum described above, and was fairly well defined since the fluorescence lifetime of 5-SLE bound to BSA was 1.8 ns. However, the ϕ of the slower component could not be defined since the fluorescence intensity had decayed to near background level at times greater than 10–15 ns. Therefore, the fluorescence anisotropy component corresponding to the EPR 30 ns component above was represented by the large r_∞ term in the exponential fit equation.

ST-EPR and phosphorescence anisotropy of 5-SLE bound to BSA in glycerol

The set of ST-EPR spectra in Fig. 5 show that as the glycerol concentration was raised (from top, 70, 75, 80;

FIGURE 3 Linear EPR spectra of 5-SLE and 5-SLE bound to BSA. The top spectrum was recorded on a sample of 20 μM 5-SLE in 5 mM sodium acetate pH 5.0 at 20°C (EPR parameters: 40 G scan width, 0.1 G modulation amplitude (peak-to-peak), 1 mW microwave power, 1024 data points). Superimposed (*dotted line*) is a simulated spectrum with a τ_r of 150 ps. The bottom spectrum was recorded on a sample of 20 μM 5-SLE/20 μM BSA in 5 mM sodium acetate pH 5.0 at 20°C (100 G scan width, 0.5 G modulation amplitude (peak-to-peak), other parameters same as above). Superimposed are two simulated spectra having τ_r values of 3 ns (*dot-dashed* line) and 30 ns (*dotted line*).

to bottom, 86%, wt/wt) at 2°C, the τ_r for the 5-SLE/BSA complex increased as a result of the increase in the solution viscosity. Superimposed on each spectrum is a computer simulation with the τ_r value given on the left. The use of spectral simulation to analyze ST-EPR data stems from the methods originally proposed by Thomas and McConnell (25). However, the computational approach employed here is based upon solution of the stochastic Liouville equation as described previously (17). Tensor values (A and g) used in the simulations were obtained by fitting the corresponding linear EPR spectrum from each sample (see Fig. 1 of accompanying paper (12)). Fig. 6 shows the statistics-of-fit (r^2) of the simulated spectra for each of the experimental spectra as a function of the τ_r. These data indicated that a high degree of confidence can be placed in the τ_r's determined by this approach.

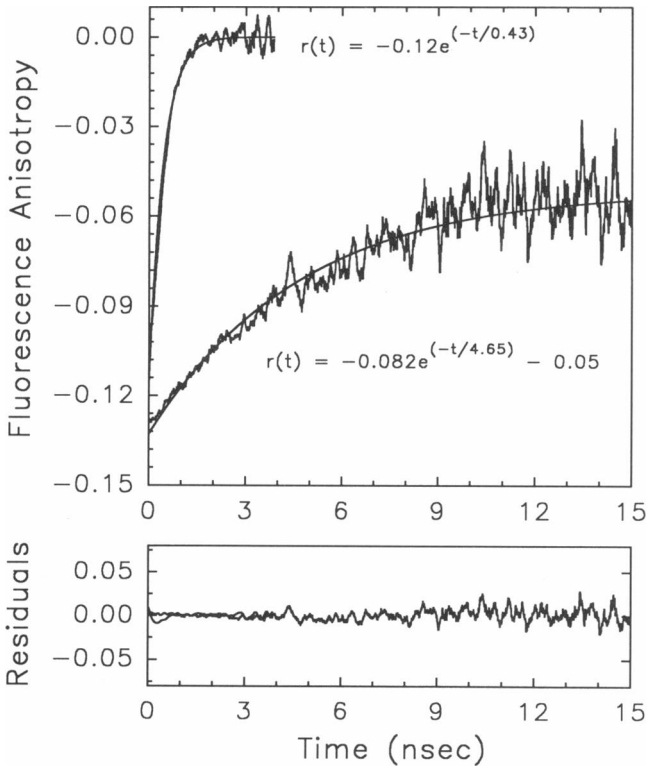

FIGURE 4 Fluorescence anisotropy decay curves of 5-SLE and 5-SLE bound to BSA. Data were collected as described in Methods, with a bin width of 6.104 ps, and summed over 20 $I_\parallel$ and $I_\perp$ polarizer data sets (60 s per set). The fast decaying anisotropy curve (data out to 3.5 ns) was recorded on a sample composed of 1.5 μM 5-SLE in 5 mM sodium acetate, pH 5.0, at 20°C. The data were fit to a single exponential equation as shown above (ϕ = 0.42 ns) with no residual anisotropy. Residuals from the fit are shown in the bottom panel. The slow decaying anisotropy curve was recorded on a sample composed of 1.5 μM 5-SLE/15 μM BSA in 5 mM sodium acetate, pH 5.0, at 20°C (a 10-fold molar excess of BSA was added to insure that all the 5-SLE was bound at this concentration). The data were also fit to a single exponential equation as shown above (ϕ = 4.7 ns) with a residual anisotropy of 0.05. The residuals from the fit are shown in the bottom panel. Both sets of data were G-factor corrected.

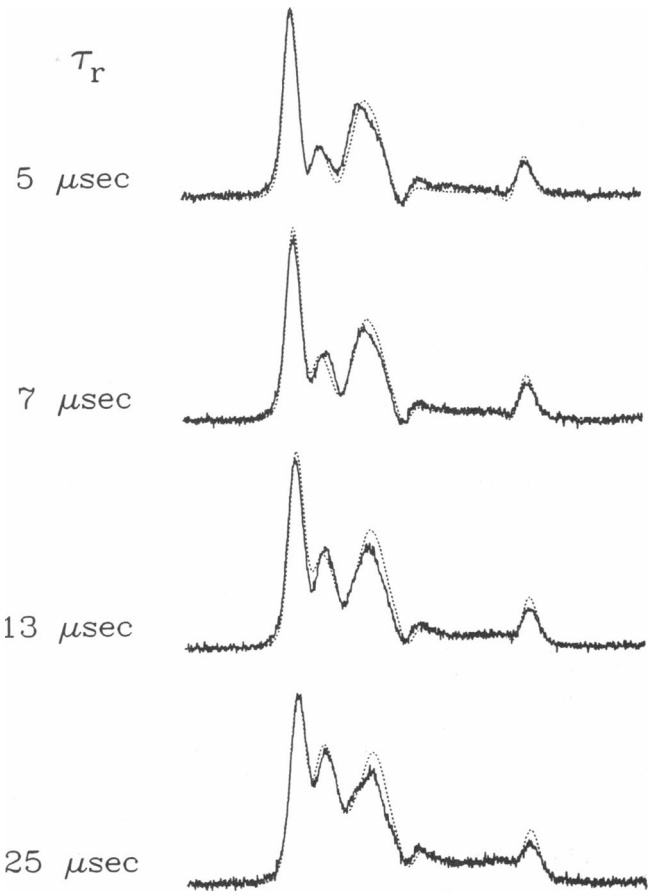

FIGURE 5 ST-EPR spectra of 5-SLE bound to BSA in glycerol at 2°C. The ST-EPR spectra (*solid lines;* second-harmonic out-of-phase absorption) were collected on samples containing 20 μM 5-SLE/20 μM BSA in 5 mM sodium acetate, pH 5.0, and 70, 75, 80, or 86 weight % glycerol (ST-EPR parameters: 100 G scan width, 5 G modulation amplitude (peak-to-peak), 100 mW microwave power, 1024 data points). Superimposed (*dotted lines*) on each experimental spectrum is a best-fit calculated spectrum (200 points) using the τ_r values given to the left. The ST-EPR lineshape from the minor 3 ns component (linear EPR component shown in Fig. 3, *dot-dashed line*) was digitally subtracted from each display prior to fitting of the data. Additional input parameters for the simulations included: A and g tensors from fit of the linear EPR spectrum (Fig. 1 of accompanying paper (12)); h_1 = 0.18 G, 0.18 G, 0.20 G and 0.22 G for the 70, 75, 80, and 86 weight % glycerol samples, respectively; T_2 = 40 ns; T_1 = 27 μs; and a post-computation Gaussian broadening of 1.4 G for each.

Fig. 7 shows the four phosphorescence anisotropy decay curves corresponding to the four ST-EPR spectra of Fig. 5. The fits superimposed on each of the decay curves consisted of two exponential terms; one of which had a very short time constant (2 μs) which remained invariant in all samples and was also present in a sample of 5-SLE without BSA (due to instrument gating response necessary to eliminate the prompt fluorescence), and a second term whose ϕ-value varied as a function of the glycerol concentration (*inset, top panel*). The residuals (*bottom panel,* Fig. 7) clearly indicated that two exponential terms adequately fit all four of the experimental data sets. Addition of a third exponential decay term did not

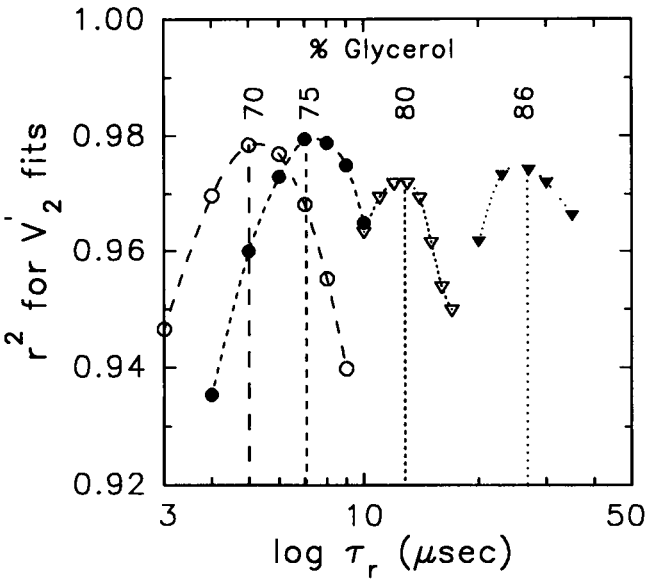

FIGURE 6 Graphical display of r^2-statistics versus τ_r for the 70, 75, 80, and 86 weight % glycerol samples. Spectra were calculated at each of the τ_r values given on the abcissa and expanded to 1024 points. The r^2-value was calculated as: $r^2 = 1 - [\Sigma (Y_e - Y_c)^2/(\Sigma (Y_e - Y_{bar})^2]$; where Y_e was the experimental amplitude, Y_c was the calculated amplitude, and Y_{bar} was the average experimental amplitude. For calculations of r^2, the baselines of the computed spectra were superimposed through the center of the noise of the experimental baseline and the amplitude of the computed spectrum adjusted to give the maximum r^2 (i.e., the best-fit of the experimental data). The fits shown in Fig. 5 all gave $r^2 > 0.972$.

result in an improved fit of the experimental data (data not shown). The total phosphorescence intensity decay of the 5-SLE-BSA adduct exhibited multi-exponential decay, the largest component (89% of the total intensity) having a lifetime of ~1,600 μs and the minor component having a lifetime of ~130 μs. For comparison, the major (90%) phosphorescence intensity decay component of unbound 5-SLE had a lifetime of ~270 μs and a minor component having a lifetime of ~95 μs (1).

The τ_r values determined from the ST-EPR spectra (*triangles*) and the phosphorescence anisotropy curves (*circles*) above are plotted versus the viscosity divided by the absolute temperature (η/T) in Fig. 8. The solid lines are determined by linear regression of the data points. According to the Stokes-Einstein relationship, the slope of the regression lines are proportional to the cube of the hydrated radius (r_h) of the 5-SLE/BSA adduct (making the approximation of isotropic rotational diffusion for BSA and that the rotation of the adduct is Brownian in nature). The r_h determined from the ST-EPR line was 30.5 Å, versus 31.6 Å determined from the phosphorescence anisotropy data. The error bars on the data points were calculated from the r^2-statistics for ST-EPR data and from the corresponding χ^2-statistics for the phosphorescence anisotropy decay fits.

DISCUSSION

A major impetus for this work was to explore the feasibility of constructing a stable dual molecular probe suitable for the full range of fluorescence, phosphorescence, and EPR measurements in order to take maximal advantage of the complementary information potentially available from these spectroscopic techniques. The data presented demonstrate that 5-SLE provides many of the requisite properties. Even though nitroxide spin-labels are generally effective collisional quenchers of fluorescent probes, the arrangement between the spin-label moiety of 5-SLE and the eosin molecular framework did not lead to significant alterations in the measured optical properties of the probe when compared with the non-paramagnetic homolog 5-acetyleosin (1).

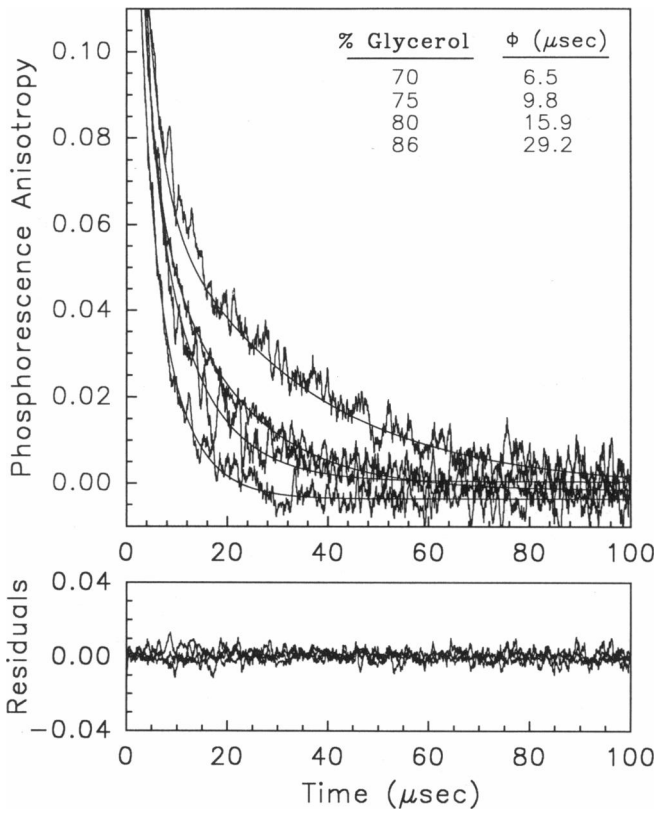

FIGURE 7 Phosphorescence anisotropy decay curves of 5-SLE bound to BSA in glycerol at 2°C. The anisotropy decay curves were collected on samples containing 1.5 μM 5-SLE/15 μM BSA in 5 mM sodium acetate, pH 5.0, and 70, 75, 80, or 86 weight % glycerol (a 10-fold molar excess of BSA was added to insure that all the 5-SLE was bound at this concentration). Samples were deoxygenated as described in Methods. Photons were collected into 15,360 40 ns-wide bins (614 μs total width) with a total of 262,144 laser pulses per $I_\parallel$ and $I_\perp$ data set (the emission polarizer was rotated after every 32,768 pulses). The anisotropy curves were fit to double exponential equations, one term having a short (2 μs) time constant which was present in a sample of unbound 5-SLE (instrument gating response), and the other term having a ϕ which was dependent on the glycerol concentration (shown in table inset, *top panel*). The bottom panel shows the residuals from all four fits. The anisotropy decay curves were G-factor corrected.

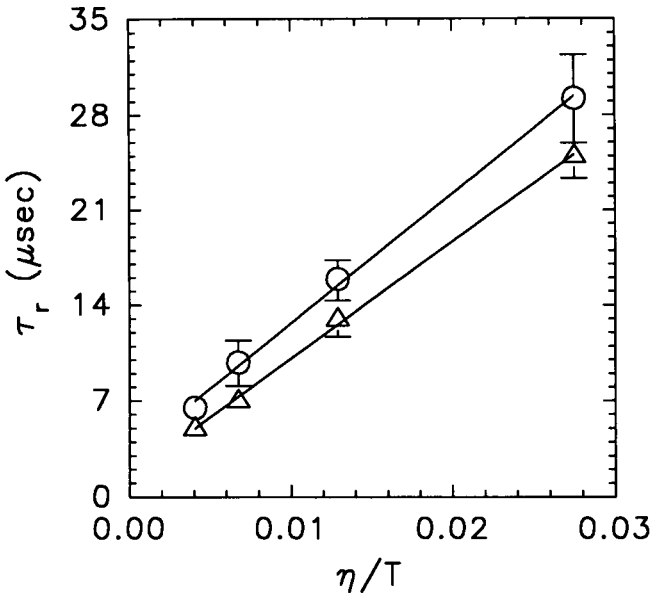

FIGURE 8 Determination of the hydrated radius of BSA from the ST-EPR and phosphorescence anisotropy data. The τ_r values determined from the ST-EPR spectra (*triangles*) and phosphorescence anisotropy (*circles;* using the approximation of isotropic rotational diffusion, $\phi = \tau_r$) are plotted versus the viscosity/temperature (±SD). The hydrated radii determined from the slope of the lines are 30.5 Å for the ST-EPR data sets and 31.6 Å for the phosphorescence data sets.

Though extensive structural work has not been carried out on 5-SLE to date, it is reasonable to assume that the amide bond formed between the spin-label and eosin will exhibit structural features similar to previously synthesized spin-label probes possessing the same chemical linkage (26). In the case of spin-labeled 3,6-diaminoacridine, the five-membered spin-label ring was tilted ~40° from the plane of the heterocyclic ring system. This geometry places the carbonyl oxygen of the amide in Van der Waals contact with one of the aromatic protons located ortho to the amide nitrogen. The potential for double-bond conjugation over this region of the molecule may provide an effective energy barrier for free rotations about the chemical bonds between the spin-label and eosin moieties. The extent to which these structural properties exist and contribute to the observed spectral properties of 5-SLE remain to be explored in greater detail.

Anecdotal and published reports (e.g., 9, 10) of spin-labeled fluorophores being synthesized and effectively quenched by the virtue of interactions between the paramagnetic center and the fluorophore suggest that this dual molecular probe approach may have limitations for some types of chemical linkages and some fluorophores. We have not explored this limitation in any systematic fashion. However, in the course of these studies we have chemically synthesized and isolated the analogous spin-labeled derivative of 5-aminofluorescein (5-SLF). Like 5-SLE, 5-SLF was observed to exhibit fluorescence properties similar to the 5-acetyl derivative of fluorescein (data not shown). By analogy, it is considered likely that the corresponding spin-label derivative of 5-aminoerythrosin would also retain its optical properties and serve as a suitable dual probe.

The spectroscopic data obtained on 5-SLE in solution (Fig. 3, *upper;* and Fig. 4, *lower* decay curve) would seem to suggest that there may be some motional freedom of the spin-label moiety relative to eosin based solely upon the effective rotational correlation times derived from fitting of the respective EPR and optical data (compare 150 ps from the EPR fit with 430 ps from the fluorescence anisotropy decay fit). However, it should be emphasized that there is considerable uncertainty in fitting of the EPR data in this correlation time range. First, the homogeneous linewidth used in the computational modeling cannot be determined from cw-EPR alone due to the inhomogeneous broadening of resonance lines by contact coupling to nitroxide ring deuterons. Next, to accurately represent the experimental line shape (i.e., the degree of Lorentzian versus Gaussian character), one would need to sum Lorentzian lines with an intensity weighting and splitting distribution consistent with nearby deuterons. Finally, an isotropic Brownian rotational diffusion model was employed to fit the experimental data. This model is likely too simplified to account for the true rotational diffusion of a relatively small and planar molecule like 5-SLE in solution. Even given these uncertainties, it is clear that the rotational freedom of the spin-label moiety of 5-SLE is severely restricted by covalent attachment to eosin since the corresponding EPR spectrum from 2,2,5,5-tetramethyl-3-pyrroline-d_{13},1-^{15}N-1-oxyl-3-carboxylic acid recorded under the same conditions exhibits two very sharp lines of nearly equal amplitude (data not shown).

When 5-SLE is bound noncovalently to BSA, the EPR spectrum clearly shows a major slow motion component (Fig. 3, *lower*). Fitting of this component yielded a correlation time of 30 ns as shown by the superimposed dotted line. From the Stokes-Einstein relationship, this rotational correlation time predicts an effective hydrated radius of 30.6 Å, which is in reasonable agreement with the hydrodynamically determined value for BSA of 33.7 Å (23). This value also compares well with the correlation time of ~40 ns for dansylated BSA as measured (time-resolved fluorescence anisotropy) by Weber (27), and values of 33 and 30.5 ns determined by time-resolved tryptophan fluorescence anisotropy of horse serum albumin (28) and rat serum albumin (29). BSA is known to be an asymmetric protein and therefore, would be predicted to exhibit different rotational correlation times about its major and minor axes (see reference 18). Since the geometric arrangement between the major axis system of the nitroxide and the inertial axis system of BSA is unknown, it is not possible to uniquely

refine the fit of the EPR data. The important point, however, is that the nitroxide moiety of 5-SLE reports with reasonable accuracy on the global tumbling of BSA. Unfortunately, it is not possible to make a direct comparison of rotational correlation times for this slow component with transient fluorescence anisotropy measurements on the 5-SLE-BSA complex in buffer due to the short fluorescence lifetime of the eosin. Although there is a τ_r time window from approximately 10^{-8} to 10^{-7} s which falls between the conventional time-resolved fluorescence and phosphorescence anisotropy decay methods used in this report, other methods such as fluorescence recovery anisotropy (30), fluorescence correlation spectroscopy (31), or fluorescence photobleaching recovery (32) could be employed with dual probes of this type which would span this time window.

In addition to the slow motion EPR component in Fig. 3, lower, there is also a minor component with intermediate mobility. Possible sources for this component include: (*a*) a separate secondary binding site for the probe, (*b*) a different conformation of 5-SLE within the same binding site, or (*c*) a restricted, but not totally immobilized, motional mode of bound 5-SLE. We have not explored the origin of this intermediate component in the present work. However, it is interesting to compare the motional characteristics of this species deduced from fitting the EPR and optical data. The superimposed dot-dashed line in Fig. 3, lower, is a calculated EPR spectrum using a correlation time of 3 ns. This value compares favorably with the 4.6 ns decay observed with transient fluorescence anisotropy in Fig. 4, *upper* decay curve.

The most rigorous comparison of EPR and optical results in the present work was provided by studies on the 5-SLE/BSA complex in glycerol/buffer solutions of variable composition. The ST-EPR data in Fig. 5 were best-fit with isotropic rotational correlation times of 5, 7, 13, and 25 μs for the 70, 75, 80, and 86 wt% glycerol samples, respectively. The r^2-statistics provided in Fig. 6 define the confidence intervals for the individual fits. These correlation times agree closely with the times of 6.5, 9.8, 15.9, and 29.2 μs determined from fitting the transient phosphorescence anisotropy decays in Fig. 7. Global simultaneous analysis of both data sets are described in the accompanying manuscript (12). Plotting of these sets of data as τ_r versus η/T (Fig. 8) allows calculation of the effective hydrated radius of the 5-SLE/BSA complex. The agreement between the values determined, 30.5 and 31.6 Å, from the ST-EPR and phosphorescence anisotropy measurements, respectively, is encouraging and provides confidence that the 5-SLE probe is accurately reporting global dynamics information via both reporter moieties.

The data presented clearly demonstrate that a single molecular probe possessing both a stable spin-label and an optical reporter moiety can be employed with standard instrumentation to make the full range of EPR, ST-EPR, fluorescence, and phosphorescence measurements, techniques which many investigators rely heavily upon when examining dynamics of macromolecular systems. Additional probes built around the molecular structure of 5-SLE but with the capability for covalent modification of proteins, nucleic acids, or other large biomolecules, where the size of the probe does not strongly influence dynamics of interest, should prove to be extremely useful in a wide range of investigations utilizing EPR and optical spectroscopies.

The authors wish to thank the mass spectrometry center at Vanderbilt for recording mass spectral data.

This work was supported in part by grants from the National Institutes of Health HL34737, CA43720, and RR04075 to A. Beth, and GM45990, RR05823, and L. P. Markey to J. Beechem. J.M.B. is a Lucille P. Markey Scholar. E. Hustedt was supported by a training grant from NIH, T32 DK07186, as a postdoctoral fellow.

Received for publication 2 September and in final form 10 November 1992.

REFERENCES

1. Beth, A. H., C. E. Cobb, and J. M. Beechem. 1992. Synthesis and characterization of a combined fluorescence, phosphorescence, and electron paramagnetic resonance probe. Society of photo-optical instrumentation engineers, time-resolved laser spectroscopy III. 504–512.
2. Ohnishi, S., and H. M. McConnell. 1965. Interaction of the radical ion of chloropromazine with deoxyribonucleic acid. *J. Am. Chem. Soc.* 87:2293.
3. Stone, T. J., T. Buckman, R. L. Nordio, and H. M. McConnell. 1965. Spin-labeled biomolecules. *Proc. Natl. Acad. Sci. USA.* 54:1010–1017.
4. Haugland, R. P. 1989. Handbook of Fluorescent Probes and Research Chemicals, Molecular Probes, Inc., Eugene, OR.
5. Thomas, D. D., T. M. Eads, V. A. Barnett, K. M. Lindahl, D. A. Momont, and T. C. Squier. 1985. Saturation transfer EPR and triplet anisotropy: complementary techniques for the study of microsecond rotational dynamics. *In* Spectroscopy and the Dynamics of Molecular Biological Systems. P. Bayley and R. Dale, editors. Academic Press, London. 239–257.
6. Ajtai, K., A. Ringler, and T. P. Burghardt. 1992. Probing cross-bridge angular transitions using multiple extrinsic reporter groups. *Biochemistry.* 31:207–217.
7. Ajtai, K., and T. P. Burghardt. 1992. Luminescent/paramagnetic probes for detecting order in biological assemblies: transformation of luminescent probes into π-radicals by photochemical reduction. *Biochemistry.* 31:4275–4282.
8. Burghardt, T. P., and K. Ajtai. 1992. Mapping global angular transitions of proteins in assemblies using multiple extrinsic reporter groups. *Biochemistry.* 31:200–206.
9. Green, S. A., D. J. Simpson, G. Zhou, P. S. Ho, and N. V. Blough. 1990. Intramolecular quenching of excited states by stable nitroxyl radicals. *J. Am. Chem. Soc.* 112:7337–7346.
10. Matko, J., K. Ohki, and M. Edidin. 1992. Luminescence quenching by nitroxide spin labels in aqueous solution: studies on the mechanism of quenching. *Biochemistry.* 31:703–711.
11. Stryer, L., and O. H. Griffith. 1965. A Spin-Labeled Hapten. *Proc. Natl. Acad. Sci. USA.* 54:1785–1791.
12. Hustedt, E. J., C. E. Cobb, A. H. Beth, and J. M. Beechem. 1992.

Measurement of rotational dynamics by the simultaneous nonlinear analysis of optical and EPR data. *Biophys. J.* 64:614–621.

13. Rozantsev, E. G. 1970. Syntheses of some stable radicals and the most important intermediates. *In* Free Nitroxyl Radicals. H. Ulrich, editor. Plenum Press, New York. 209–210.
14. Cobb, C. E., and A. H. Beth. 1990. Identification of the eosinyl-5-maleimide reaction site on the human erythrocyte anion-exchange protein: overlap with the reaction sites of other chemical probes. *Biochemistry.* 29:8283–8290.
15. Cobb, C. E., S. Juliao, K. Balasubramanian, J. V. Staros, and A. H. Beth. 1990. Effects of diethyl ether on membrane lipid ordering and on rotational dynamics of the anion exchange protein in intact human erythrocytes: correlations with anion exchange function. *Biochemistry.* 29:10799–10806.
16. Beth, A. H., K. Balasubramanian, B. H. Robinson, L. R. Dalton, S. D. Venkataramu, and J. H. Park. 1983. Sensitivity of V_2' saturation transfer electron paramagnetic resonance signals to anisotropic rotational diffusion with [^{15}N]nitroxide spin labels: effects of noncoincident magnetic and diffusion tensor principal axes. *J. Phys. Chem.* 87:359–367.
17. Robinson, B. H., H. Thomann, A. H. Beth, P. Fajer, and L. R. Dalton. 1985. EPR and Advanced EPR Studies of Biological Systems. CRC Press, Boca Raton, FL. 314 pp.
18. Beth, A. H., and B. H. Robinson. 1989. Nitrogen-15 and deuterium substituted spin labels for studies of very slow rotational motion. *In* Biological Magnetic Resonance VIII. L. J. Berliner and J. Reubin, editors. Plenum Press, New York. 179–253.
19. Eads, T. M., D. D. Thomas, and R. H. Austin. 1984. Microsecond rotational motions of eosin-labeled myosin measured by time-resolved anisotropy of absorption and phosphorescence. *J. Mol. Biol.* 179:55–81.
20. Beechem, J. M., E. Gratton, M. Ameloot, J. R. Knutson, and L. Brand. 1991. The global analysis of fluorescence intensity and anisotropy decay data: second generation theory and programs. *In* Topics in Fluorescence Spectroscopy, Vol. 2. J. R. Lackowicz, editor. Plenum Press, New York. 241–305.
21. Beechem, J. M. 1992. Global analysis of biochemical and biophysical data. *Methods. Enzymol.* 210:37–54.
22. Cherry, R. J., A. Cogoli, M. Oppliger, G. Schneider, and G. Semenza. 1976. A spectroscopic technique for measuring slow rotational diffusion of macromolecules. 1. Preparation and properties of a triplet probe. *Biochemistry.* 15:3653–3656.
23. Tanford, C. 1961. Physical Chemistry of Macromolecules. John Wiley & Sons, New York. 395pp.
24. Fleming, G. R., J. M. Morris, and G. W. Robinson. 1976. Direct observation of rotational diffusion by picosecond spectroscopy. *Chem. Phys.* 17:91–100.
25. Thomas, D. D., and H. M. McConnell. 1974. Calculation of paramagnetic resonance spectra sensitive to very slow rotational motion. *Chem. Phys. Lett.* 25:470–475.
26. Robinson, B. H., L. S. Lerman, A. H. Beth, H. L. Frisch, L. R. Dalton, and C. Auer. 1980. Analysis of double-helix motions with spin-labeled probes: binding geometry and the limit of torsional elasticity. *J. Mol. Biol.* 139:19–44.
27. Weber, G. 1952. Polarization of the fluorescence of macromolecules 2. Fluorescent conjugates of ovalbumin and bovine serum albumin. *Biochem. J.* 51:155–167.
28. Vos, K., A. van Hoek, and A. J. Visser. 1987. Application of a reference convolution method to tryptophan fluorescence in proteins: a refined description of rotational dynamics. *Eur. J. Biochem.* 165:55–63.
29. Gentin, M., M. Vincent, J-C. Brochon, A. Livesey, N. Cittanova, and J. Gallay. 1990. Time-resolved fluorescence of the single tryptophan residue in rat α-fetoprotein and rat serum albumin: analysis by the maximum-entropy method. *Biochemistry.* 29:10405–10412.
30. Corin, A. F., E. Blatt, and T. M. Jovin. 1987. Triplet-state detection of labeled proteins using fluorescence recovery spectroscopy. *Biochemistry.* 26:2207–2217.
31. Ehrenberg, M., and R. Rigler. 1976. Fluorescence correlation spectroscopy applied to rotational diffusion of macromolecules. *Q. Rev. Biophys.* 9:69–79.
32. Wegener, W., and R. Rigler. 1984. Separation of translational and rotational contributions in solution studies using fluorescence photobleaching recovery. *Biophys. J.* 46:787–793.